Matter and Radiation at Extremes | RESEARCH ARTICLE | scitation.org/journal/mre

Pressure-induced reemergence of superconductivity in $BaIr_2Ge_7$ and $Ba_3Ir_4Ge_{16}$ with cage structures

Cite as: Matter Radiat. Extremes 7, 038404 (2022); doi: 10.1063/5.0088235
Submitted: 14 February 2022 • Accepted: 14 April 2022 •
Published Online: 11 May 2022

Cuiying Pei,[1] Tianping Ying,[2,a)] Yi Zhao,[1] Lingling Gao,[1] Weizheng Cao,[1] Changhua Li,[1] Hideo Hosono,[3] and Yanpeng Qi[1,4,5,a)]

AFFILIATIONS

[1] School of Physical Science and Technology, ShanghaiTech University, Shanghai 201210, China
[2] Beijing National Laboratory for Condensed Matter Physics, Institute of Physics, Chinese Academy of Sciences, Beijing 100190, China
[3] Materials Research Center for Element Strategy, Tokyo Institute of Technology, Yokohama 226-8503, Japan
[4] ShanghaiTech Laboratory for Topological Physics, ShanghaiTech University, Shanghai 201210, China
[5] Shanghai Key Laboratory of High-Resolution Electron Microscopy, ShanghaiTech University, Shanghai 201210, China

[a)] **Authors to whom correspondence should be addressed:** ying@iphy.ac.cn and qiyp@shanghaitech.edu.cn

ABSTRACT

Clathrate-like or caged compounds have attracted great interest owing to their structural flexibility, as well as their fertile physical properties. Here, we report the pressure-induced reemergence of superconductivity in $BaIr_2Ge_7$ and $Ba_3Ir_4Ge_{16}$, two new caged superconductors with two-dimensional building blocks of cage structures. After suppression of the ambient-pressure superconducting (SC-I) states, new superconducting (SC-II) states emerge unexpectedly, with T_c increased to a maximum of 4.4 and 4.0 K for $BaIr_2Ge_7$ and $Ba_3Ir_4Ge_{16}$, respectively. Combined with high-pressure synchrotron x-ray diffraction and Raman measurements, we propose that the reemergence of superconductivity in these caged superconductors can be ascribed to a pressure-induced phonon softening linked to cage shrinkage.

I. INTRODUCTION

The recent discovery of superconductivity in LaH_{10} at high pressure with record-high superconducting transition temperatures T_c ~ 260 K has fueled the search for room-temperature superconductivity in compressed superhydrides.[1–3] The three-dimensional clathrate-like structure of H with La atoms filling the clathrate cavities has been described as an extended metallic hydrogen host structure stabilized by the La as a guest electron donor. The introduction of electrons into H_2 molecules by the guest atom leads to a significant contribution of H to the electronic density of states at the Fermi level. As a result, substantial coupling of electrons on the Fermi surface with high-frequency phonons in response to the motion of the H atoms is crucial for promoting superconductivity.[4–7] Actually, clathrate-like superhydrides with alkaline-earth or other rare-earth atoms have also been proposed as potential high-T_c superconductors.[8,9] Following their theoretical prediction, experimental progress on the synthesis of these clathrate superhydrides has been remarkable: YH_6,[10,11] YH_9,[10,12] ThH_9,[13] ThH_{10},[13] CeH_9,[14,15] CeH_{10},[16] $(LaY)H_6$,[17] $(LaY)H_{10}$,[17,18] and CaH_6,[19] with high T_c values in the range of 146–253 K, have been synthesized. Thus, a new class of high-temperature superconductors with clathrate-like structure has been born.

The creation of a distinctive H clathrate structure incorporating metal inside the voids is the key to the unusually high-T_c superconductivity. Aside from hydrogen clathrate cages, the host–guest and interframework interactions are also significant in influencing superhydride superconductivity. Until now, the experimentally obtained high-temperature superconducting clathrate superhydrides have only existed above megabar pressures. The ultrahigh

pressure required to synthesize and maintain these clathrate superhydrides impedes their experimental investigation. Alternatively, several clathrate or caged compounds exhibit a superconducting transition at ambient pressure, which provides a platform to examine the relationship between guest atom and cage unit under comparatively benign conditions.[20–27] In this work, we utilize an *in situ* high-pressure method to systematically investigate the evolution of superconductivity for two Ba-filled cage compounds $BaIr_2Ge_7$ and $Ba_3Ir_4Ge_{16}$. We discover that the first superconducting phase in both caged compounds is gradually suppressed under pressure. At a higher pressure, a pressure-induced superconducting phase dome emerges. No structural phase transition is revealed by high-pressure synchrotron x-ray diffraction (XRD). The pressure-induced reemergence of superconductivity in $BaIr_2Ge_7$ and $Ba_3Ir_4Ge_{16}$ can be attributed to phonon softening, which is related to shrinkage of the cage.

II. EXPERIMENTAL

Polycrystalline $BaIr_2Ge_7$ and $Ba_3Ir_4Ge_{16}$ were prepared from stoichiometric amounts of high-purity elements by argon arc melting and subsequent annealing in evacuated quartz capsules at 1000 °C for 20 h.[23] The superconducting transition was confirmed by magnetization measurements using a Magnetic Property Measurement System (MPMS). *In situ* high-pressure resistivity measurements were conducted on a nonmagnetic diamond anvil cell (DAC) as described elsewhere.[28–32] A piece of nonmagnetic BeCu was used as the gasket. A cubic boron nitride (BN)/epoxy mixture layer was inserted between the BeCu gasket and the electrical leads as an insulator layer. Four Pt foils were arranged according to the van der Pauw method. *In situ* high-pressure XRD measurements were performed at beamline BL15U of the Shanghai Synchrotron Radiation Facility with an x-ray wavelength λ = 0.6199 Å. A symmetric DAC with 200 μm culet was used with a rhenium gasket. Silicone oil was used as the pressure-transmitting medium (PTM), and the pressure was determined by the ruby luminescence method.[33] Two-dimensional diffraction images were analyzed using FIT2D software.[34] Rietveld refinements of crystal structures under high pressure were performed using the General Structure Analysis System (GSAS) and the graphical user interface EXPGUI.[35,36] An *in situ* high-pressure Raman spectroscopy investigation of $BaIr_2Ge_7$ and $Ba_3Ir_4Ge_{16}$ was performed using a Raman spectrometer (Renishaw in-Via, UK) with a laser excitation wavelength of 532 nm and a low-wavenumber filter.

For $BaIr_2Ge_7$, we carried out high-pressure *in situ* synchrotron XRD, Raman, and transport measurements. To confirm the emergence of a second superconducting state under high pressure, we repeated the measurements with new samples for a second run. For $Ba_3Ir_4Ge_{16}$, we carried out high-pressure *in situ* Raman measurements and transport measurements in two runs.

III. RESULTS AND DISCUSSION

At ambient pressure, both $BaIr_2Ge_7$ and $Ba_3Ir_4Ge_{16}$ exhibit typically metallic behavior and show superconducting transitions at 2.7 and 5.9 K, respectively (Fig. S1, supplementary material).[23–25] Hence, we measured the electrical resistivity $\rho(T)$ for both compounds at various pressures. Figures 1(a)–1(c) present the temperature dependence of the resistivity of $BaIr_2Ge_7$ at various pressure up to 44.9 GPa. The resistivity of $BaIr_2Ge_7$ exhibits a nonmonotonic evolution with increasing pressure. Over the whole temperature range, the resistivity is first suppressed with applied pressure, reaching a minimum value at about 15 GPa, and then displays the opposite trend with further increasing pressure. In the lower-pressure region, the superconducting transition temperature T_c is suppressed to a minimum of 2.1 K at 16.7 GPa. Surprisingly, T_c starts to increase rapidly with further increases in pressure above 20 GPa, reaching a maximum value of 4.4 K at 39.7 GPa. With still further increases in pressure, T_c slowly decreases to form a complete dome shape. Compared with the value of 2.7 K at ambient pressure, T_c in the high-pressure region is much enhanced. The measurements on different samples of $BaIr_2Ge_7$ for independent runs gave consistent and reproducible results (Fig. S2, supplementary material), confirming the intrinsic superconductivity under pressure. The pressure-induced reentrant superconductivity resembles the situation in a variety of compounds, including $K_xFe_{2-y}Se_2$,[37] $(Li_{1-x}Fe_x)OHFe_{1-y}Se$,[38] $K_2Mo_3As_3$,[39] $Sr_{0.065}Bi_2Se_3$,[40] and CsV_3Sb_5.[30,41–43] In addition, we performed transport measurements on $Ba_3Ir_4Ge_{16}$ under high pressure, and a similar evolution of $\rho(T)$ was observed, as shown in Figs. 2(a), 2(b), and S3 (supplementary material). In the first superconducting region (SC-I), the application of pressure rapidly suppresses T_c below 2 K at ~20 GPa. In the second superconducting region (SC-II), T_c continuously increases to its highest value of 4.0 K at around 30 GPa, which is slightly lower than that in the SC-I region. Beyond this pressure, T_c decreases very slowly and exhibits a typical dome-like feature. The details are summarized in Table I.

To confirm whether the new resistance drop observed in $BaIr_2Ge_7$ is related to a superconducting transition, we applied a magnetic field to samples subjected to 3.8 and 44.9 GPa, respectively [Figs. 1(d) and 1(e)]. As can be seen in Fig. 1(e), this new drop in resistance shifts to a lower temperature with increasing magnetic field and is fully suppressed under a magnetic field of 2.25 T at 44.9 GPa. These results indicate that the sharp drop in resistance is a superconducting transition. We also measured the H-dependent superconducting transition under P = 3.8 GPa, and the curves are plotted in Fig. 1(d). We extract the field (H) dependence of T_c for $BaIr_2Ge_7$ at 3.8 and 44.9 GPa and plot $H(T_c)$ in Fig. 1(f). The experimental data are fitted using the Ginzburg–Landau (G-L) formula[44,45] $H_{c2}(T) = H_{c2}(0)\frac{1-t^2}{1+t^2}$, where $t = T/T_c$ is the normalized temperature, which allows us to estimate critical fields $\mu_0 H_{c2} \sim 2.3$ and 2.2 T for 3.8 and 44.9 GPa, respectively. Although the $\mu_0 H_{c2}$ obtained here is lower than its corresponding Pauli paramagnetic limit $\mu_0 H_P = 1.84 T_c$, the slopes of dH_{c2}/dT are notably different: −1.08 and −0.61 T/K for 3.8 and 44.9 GPa, respectively. Our results suggest that the nature of the pressure-induced reentrant superconducting state may differ from that of the initial superconducting state. A similar evolution of $\mu_0 H_{c2}$ is obtained for $Ba_3Ir_4Ge_{16}$ under various pressures and is shown in Figs. 2(c), 2(d), and S3 (supplementary material).

To investigate whether the observed reemergence of superconductivity in pressurized $BaIr_2Ge_7$ and $Ba_3Ir_4Ge_{16}$ is associated with a pressure-induced crystal structure phase transition, we performed *in situ* high-pressure XRD measurements. At ambient pressure, $BaIr_2Ge_7$ possesses an orthorhombic structure belonging to the

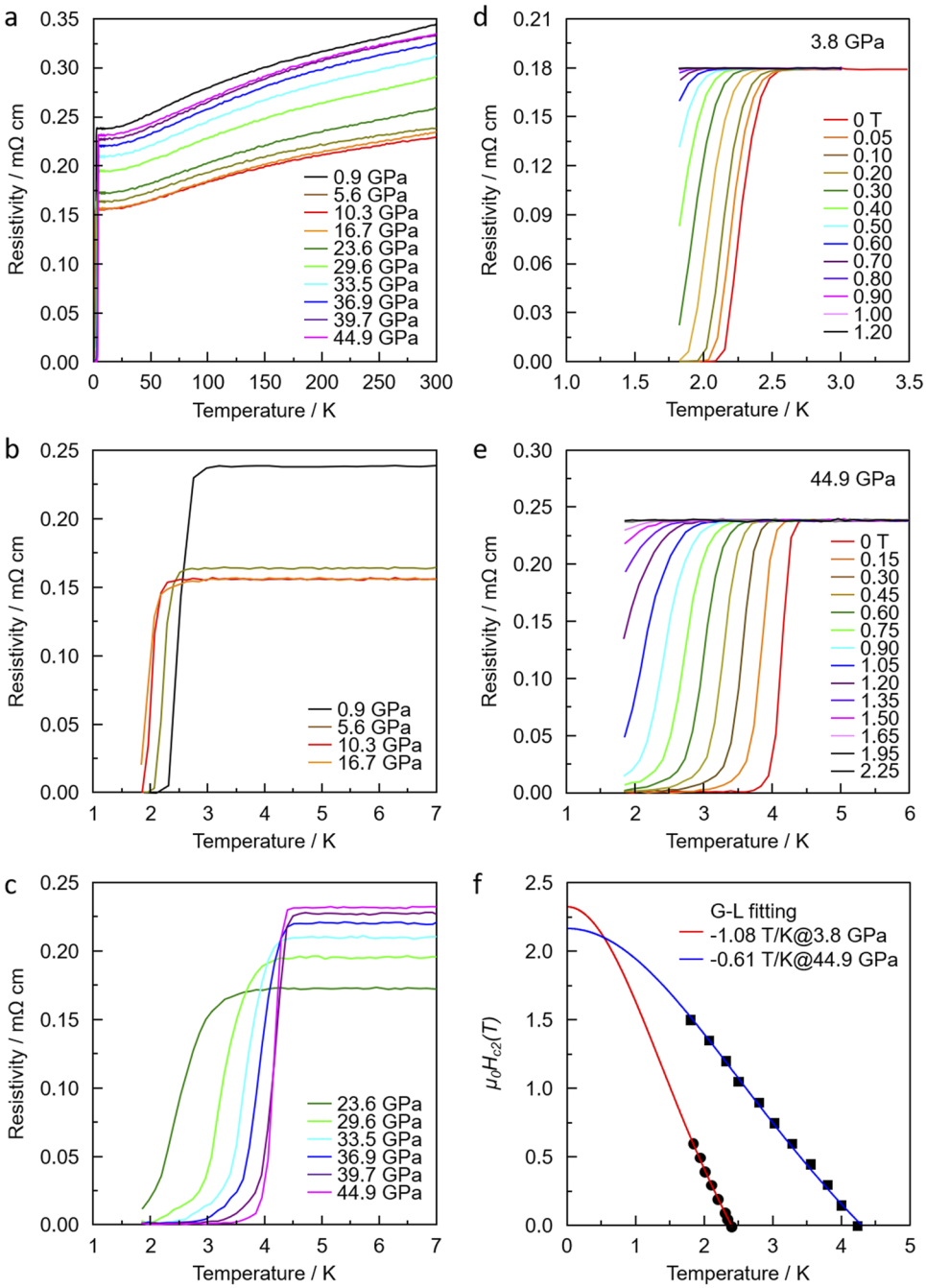

FIG. 1. (a) Electrical resistivity of $BaIr_2Ge_7$ as a function of temperature at various pressures in run I. (b) and (c) Temperature-dependent resistivity of $BaIr_2Ge_7$ in the vicinity of the superconducting transition. Temperature dependence of resistivity under different magnetic fields for $BaIr_2Ge_7$ at 3.8 (d) and 44.9 GPa (e), respectively. (f) Estimated upper critical field for $BaIr_2Ge_7$. Here, T_c is determined as a 90% drop in the normal-state resistivity. The solid lines represent fits based on the Ginzburg–Landau (G-L) formula.

space group, *Ammm*, while $Ba_3Ir_4Ge_{16}$ crystallizes into a tetragonal lattice with space group I4/*mmm* [Fig. 3(a)]. Both compounds are composed of two-dimensional networks of cage units, where $[Ir_8Ge_{16}]^{2-}$ cages are connected by $[Ir_2Ge_{16}]^{2-}$ cages encapsulating barium atoms. The XRD patterns of $BaIr_2Ge_7$ collected at different pressures are shown in Fig. 3(b). A representative refinement at 0.3 GPa is displayed in Fig. S4 (supplementary material). All the diffraction peaks can be indexed well to the ambient structure. With increasing pressure, all peaks shift to a higher angle owing to shrinkage of the lattice, and no structural phase transition is observed under pressures up to 60.5 GPa. Structural refinements have been carried out by Rietveld analysis using synchrotron XRD patterns, and the unit-cell lattice parameters as functions of pressure have been extracted as depicted in Fig. S5(c) (supplementary material). It

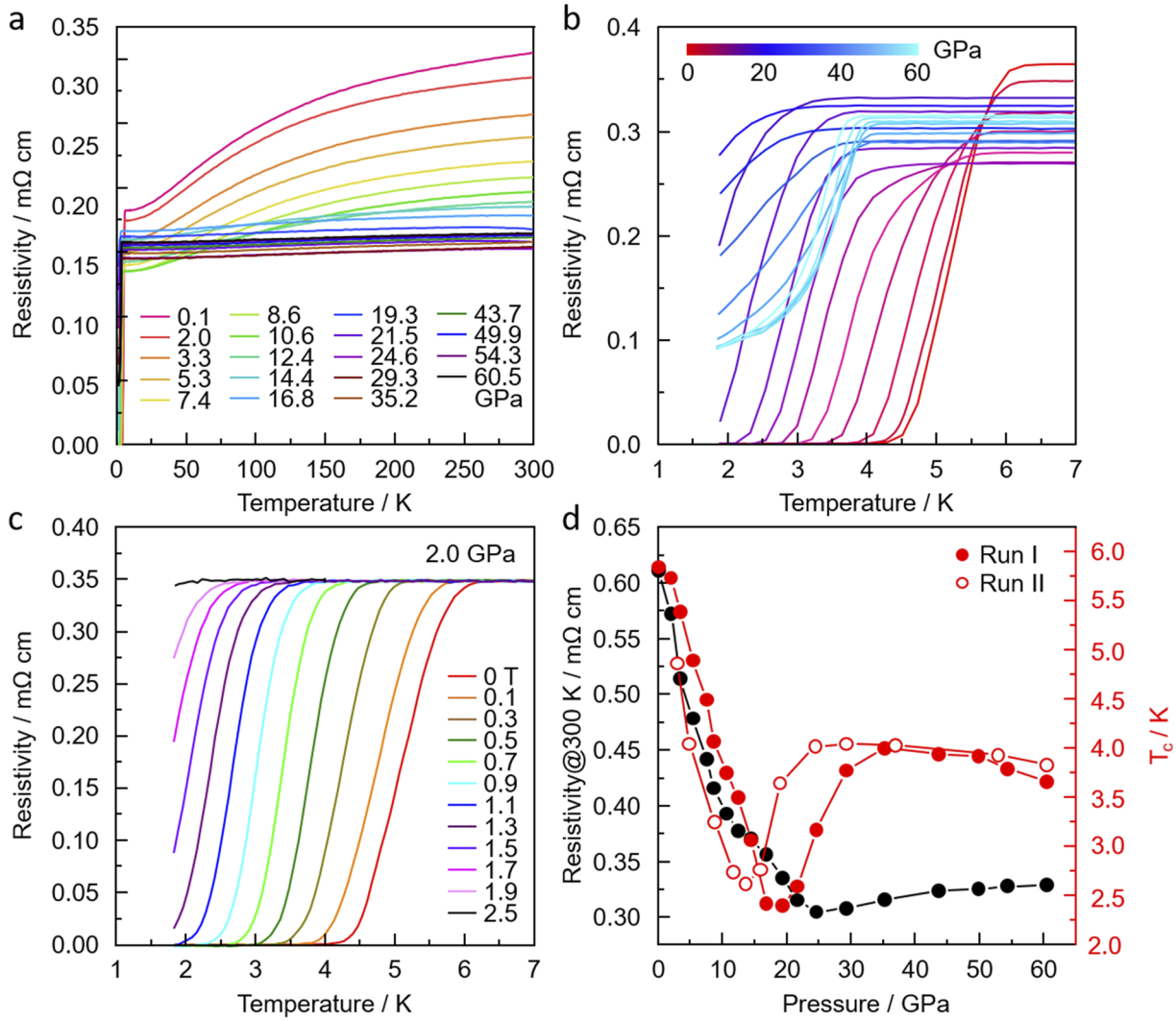

FIG. 2. (a) Electrical resistivity of $Ba_3Ir_4Ge_{16}$ as a function of temperature at various pressures in run I. (b) Temperature-dependent resistivity of $Ba_3Ir_4Ge_{16}$ in the vicinity of the superconducting transition. (c) Temperature dependence of resistivity under different magnetic fields for $Ba_3Ir_4Ge_{16}$ at 2.0 GPa. (d) Pressure-dependent resistivity at 300 K and T_c of $Ba_3Ir_4Ge_{16}$.

TABLE I. Structure and superconducting properties of $BaIr_2Ge_7$ and $Ba_3Ir_4Ge_{16}$.

Sample	Structure	Space group	State	T_{cmax} (K)	H_{c2} (T)
$BaIr_2Ge_7$	Orthorhombic	*Ammm*	SC-I SC-II	2.7 at 0.6 GPa 4.4 at 39.7 GPa	2.3 at 3.8 GPa 2.2 at 44.9 GPa
$Ba_3Ir_4Ge_{16}$	Tetragonal	I4/*mmm*	SC-1 SC-II	5.8 at 0.1 GPa 4.0 at 35.2 GPa	2.0 at 2.0 GPa 1.7 at 60.5 GPa

is found that the lattice constants shrink obviously at the beginning, while decreasing slowly at high pressure.

We summarize the transport results for $BaIr_2Ge_7$ in a pressure–temperature phase diagram [Fig. 4(a)]. To confirm the emergence of a second superconducting state under high pressure, we repeated the measurements with new samples for a second run and proved that all the results are reproducible. The superconducting T_c shows a similar trend to the normal resistivity. The P–T_c

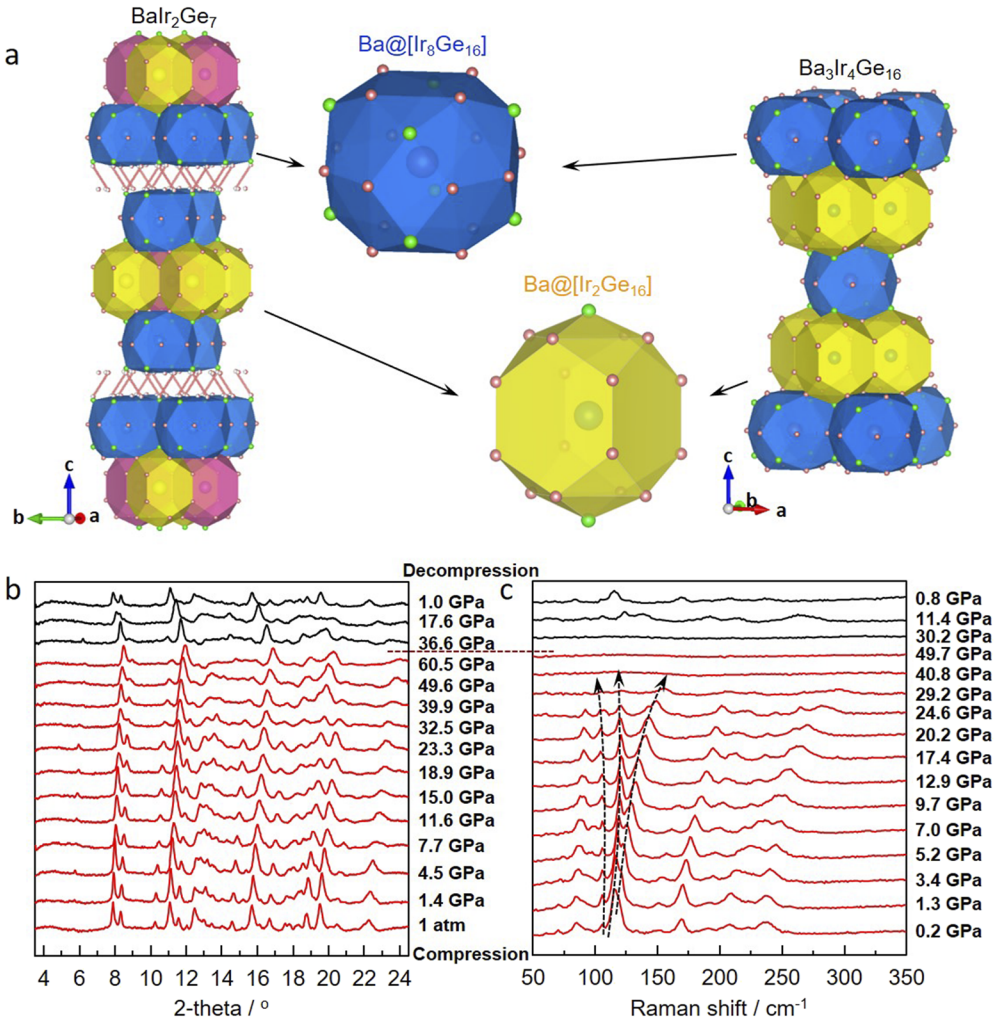

FIG. 3. (a) Crystal structures of $BaIr_2Ge_7$ and $Ba_3Ir_4Ge_{16}$. Polyhedra of different colors stand for distinct cages. (b) XRD patterns collected at various pressures for $BaIr_2Ge_7$ with an x-ray wavelength $\lambda = 0.6199$ Å (background-subtracted). (c) Selected Raman spectra at various pressure for $BaIr_2Ge_7$.

phase diagram reveals two distinct superconducting regions: the initial superconducting state (SC-I) and the pressure-induced superconducting state (SC-II). In the SC-I region between 1 bar and 16 GPa, T_c is monotonically suppressed with external pressure, and T_c can be suppressed to 2 K at around 16 GPa. In the SC-II region, T_c increases with pressure and shows a dome shape with the maximum $T_c \sim 4.4$ K at 40 GPa.

The pressure dependence of volume is shown in Fig. 4(b). With increasing pressure, one can see that the volume decreases, but with different slopes below and above a critical pressure $P_c \sim 16$ GPa. A Birch–Murnaghan equation of state was used to fit the measured pressure–volume (P–V) data for $BaIr_2Ge_7$.[46] The obtained bulk modulus K_0 is 116(2) GPa with $V_0 = 1545(1)$ Å^3 and $K_0' = 4$. However, the structure becomes less compressible, with a higher bulk modulus of 238(3) GPa, when the pressure is higher than P_c. It should be noted that a pressure-induced reentrant superconducting state was observed above the critical pressure P_c. The *in situ* high-pressure XRD results indicate that the reemergence of superconductivity in $BaIr_2Ge_7$ is not associated with a crystal structure phase transition.

Although pressure-induced reemergence of superconductivity has been reported in various materials, the origin of the second SC dome is still an enigma. A structural phase transition is usually responsible for two-dome superconductivity. However, since no structural transition was observed from our synchrotron XRD up to 60 GPa, this mechanism can be ruled out for $BaIr_2Ge_7$. Another explanation is associated with the competition or coexistence of some order parameters (e.g., charge-density waves, spin-density waves, or antiferromagnetic order) with superconductivity. Since no charge or magnetic orders have been reported in this caged family, charge or antiferromagnetic fluctuations turn out to be irrelevant to the two-dome superconductivity in $BaIr_2Ge_7$. Considering the caged

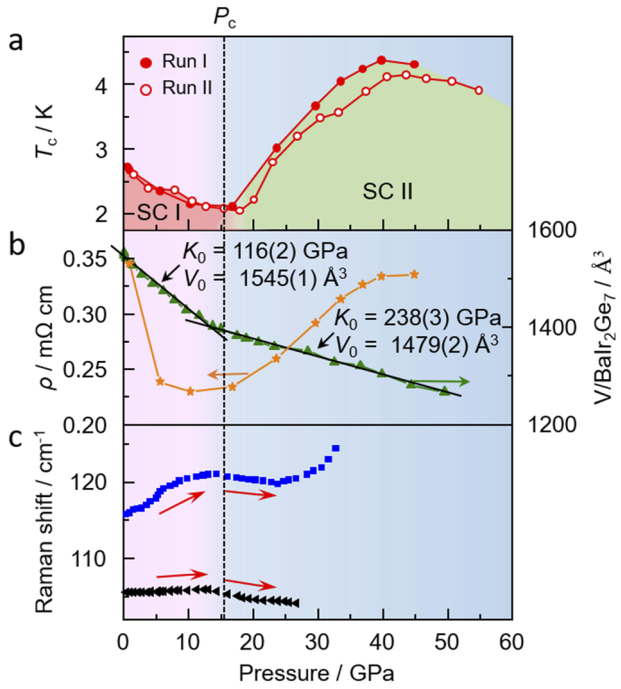

FIG. 4. Pressure dependences of (a) the superconducting transition temperatures T_c, (b) the resistivity at 300 K and the experimental volume relative to the *Ammm* phase, and (c) selected Raman shifts for $BaIr_2Ge_7$. The values of T_c were determined from the high-pressure resistivity.

structure, local vibration due to rattling of the Ba atom coupled with low-frequency phonons and conductive electrons may be responsible for superconductivity. Typically, the low-lying excitation state from the rattling guest atom in the cage can be systemically tuned by external pressure. To gain a more detailed understanding of reemergent superconducting behavior, we performed high-pressure *in situ* Raman spectroscopy measurements on $BaIr_2Ge_7$. With increasing pressure, the profile of the spectra remains similar to that at ambient pressure, and the observed modes exhibit a blue shift, which is typical behavior under high pressure [Fig. 3(c)]. Interestingly, some typical vibrational modes (e.g., 105.6 and 115.8 cm^{-1} under ambient condition) display the opposite trend and show redshift behavior when the pressure is raised to P_c. As summarized in Fig. 4, the suppression of superconductivity in SC-I is accompanied by blue shifting of the Raman peaks, reaching a minimum T_c and maximum Raman shifts at a turning point of 12 GPa. As the pressure is further increased, both modes of the Raman shift steadily decline with increasing T_c in SC-II. We call for theoretical investigations to determine the origin of these specific vibrational modes. Similar behavior is also observed in $Ba_3Ir_4Ge_{16}$ (Fig. S6, supplementary material). Calculations such as electron–phonon coupling (EPC) analysis are very tempting to decipher this anomalous phenomenon. Nevertheless, the present results signify an intimate relationship between the Raman shift and superconductivity, and pressure-induced phonon softening may be responsible for the reemergence of superconductivity in $BaIr_2Ge_7$.

In conclusion, pressure-induced reemergence of superconductivity has been observed in the caged superconductors $BaIr_2Ge_7$ and $Ba_3Ir_4Ge_{16}$. The SC-I state is initially suppressed by pressure, and then a second SC dome (SC-II) emerges, with maximum T_c ~ 4.4 and 4.0 K for $BaIr_2Ge_7$ and $Ba_3Ir_4Ge_{16}$, respectively. Synchrotron XRD measurements demonstrate that the reemergence of superconductivity is not associated with any crystal structure phase transition. In combination with *in situ* Raman measurements, our findings suggest that the development of the SC-II state in both caged compounds is a consequence of pressure-induced phonon softening caused by cage shrinkage.

SUPPLEMENTARY MATERIAL

Temperature-dependent magnetic susceptibility at ambient pressure, electrical transport in run II, typical Rietveld refinements, pressure-dependent lattice parameters and high-pressure Raman spectra are available in the supplementary material.

ACKNOWLEDGMENTS

This work was supported by the National Natural Science Foundation of China (Grant Nos. U1932217, 11974246, and 12004252), the National Key R&D Program of China (Grant No. 2018YFA0704300), the Natural Science Foundation of Shanghai (Grant No. 19ZR1477300), the Science and Technology Commission of Shanghai Municipality (Grant No. 19JC1413900), and the Shanghai Science and Technology Plan (Grant No. 21DZ2260400). The authors are grateful for support from the Analytical Instrumentation Center (Grant No. SPST-AIC10112914), SPST, ShanghaiTech University. The authors thank the staff from BL15U1 at the Shanghai Synchrotron Radiation Facility for assistance during data collection.

AUTHOR DECLARATIONS

Conflict of Interest

The authors have no conflicts to disclose.

DATA AVAILABILITY

The authors declare that the data supporting the findings of this study are available within the article and its supplementary material and are also available from the corresponding author upon reasonable request.

REFERENCES

[1] A. P. Drozdov, P. P. Kong, V. S. Minkov, S. P. Besedin, M. A. Kuzovnikov, S. Mozaffari, L. Balicas, F. F. Balakirev, D. E. Graf, V. B. Prakapenka, E. Greenberg, D. A. Knyazev, M. Tkacz, and M. I. Eremets, "Superconductivity at 250 K in lanthanum hydride under high pressures," Nature **569**(7757), 528 (2019).
[2] M. Somayazulu, M. Ahart, A. K. Mishra, Z. M. Geballe, M. Baldini, Y. Meng, V. V. Struzhkin, and R. J. Hemley, "Evidence for superconductivity above 260 K in lanthanum superhydride at megabar pressures," Phys. Rev. Lett. **122**(2), 027001 (2019).
[3] F. Hong, L. Yang, P. Shan, P. Yang, Z. Liu, J. Sun, Y. Yin, X. Yu, J. Cheng, and Z. Zhao, "Superconductivity of lanthanum superhydride investigated using the standard four-probe configuration under high pressures," Chin. Phys. Lett. **37**(10), 107401 (2020).
[4] X. Zhang, Y. Zhao, F. Li, and G. Yang, "Pressure-induced hydride superconductors above 200 K," Matter Radiat. Extremes **6**(6), 068201 (2021).

[5]V. Struzhkin, B. Li, C. Ji, X.-J. Chen, V. Prakapenka, E. Greenberg, I. Troyan, A. Gavriliuk, and H.-k. Mao, "Superconductivity in La and Y hydrides: Remaining questions to experiment and theory," Matter Radiat. Extremes **5**(2), 028201 (2020).
[6]D. Wang, Y. Ding, and H.-K. Mao, "Future study of dense superconducting hydrides at high pressure," Materials **14**, 7563 (2021); arXiv:2112.09862.
[7]J. Lv, Y. Sun, H. Liu, and Y. Ma, "Theory-orientated discovery of high-temperature superconductors in superhydrides stabilized under high pressure," Matter Radiat. Extremes **5**(6), 068101 (2020).
[8]J. A. Flores-Livas, L. Boeri, A. Sanna, G. Profeta, R. Arita, and M. Eremets, "A perspective on conventional high-temperature superconductors at high pressure: Methods and materials," Phys. Rep. **856**, 1–78 (2020).
[9]D. V. Semenok, I. A. Kruglov, I. A. Savkin, A. G. Kvashnin, and A. R. Oganov, "On distribution of superconductivity in metal hydrides," Curr. Opin. Solid State Mater. Sci. **24**(2), 100808 (2020).
[10]P. Kong, V. S. Minkov, M. A. Kuzovnikov, A. P. Drozdov, S. P. Besedin, S. Mozaffari, L. Balicas, F. F. Balakirev, V. B. Prakapenka, S. Chariton, D. A. Knyazev, E. Greenberg, and M. I. Eremets, "Superconductivity up to 243 K in the yttrium-hydrogen system under high pressure," Nat. Commun. **12**(1), 5075 (2021).
[11]I. A. Troyan, D. V. Semenok, A. G. Kvashnin, A. V. Sadakov, O. A. Sobolevskiy, V. M. Pudalov, A. G. Ivanova, V. B. Prakapenka, E. Greenberg, A. G. Gavriliuk, I. S. Lyubutin, V. V. Struzhkin, A. Bergara, I. Errea, R. Bianco, M. Calandra, F. Mauri, L. Monacelli, R. Akashi, and A. R. Oganov, "Anomalous high-temperature superconductivity in YH_6," Adv. Mater. **33**(15), 2006832 (2021).
[12]E. Snider, N. Dasenbrock-Gammon, R. McBride, X. Wang, N. Meyers, K. V. Lawler, E. Zurek, A. Salamat, and R. P. Dias, "Synthesis of yttrium superhydride superconductor with a transition temperature up to 262 K by catalytic hydrogenation at high pressures," Phys. Rev. Lett. **126**(11), 117003 (2021).
[13]D. V. Semenok, A. G. Kvashnin, A. G. Ivanova, V. Svitlyk, V. Y. Fominski, A. V. Sadakov, O. A. Sobolevskiy, V. M. Pudalov, I. A. Troyan, and A. R. Oganov, "Superconductivity at 161 K in thorium hydride ThH_{10}: Synthesis and properties," Mater. Today **33**, 36–44 (2020).
[14]X. Li, X. Huang, D. Duan, C. J. Pickard, D. Zhou, H. Xie, Q. Zhuang, Y. Huang, Q. Zhou, B. Liu, and T. Cui, "Polyhydride CeH_9 with an atomic-like hydrogen clathrate structure," Nat. Commun. **10**(1), 3461 (2019).
[15]N. P. Salke, M. M. Davari Esfahani, Y. Zhang, I. A. Kruglov, J. Zhou, Y. Wang, E. Greenberg, V. B. Prakapenka, J. Liu, A. R. Oganov, and J.-F. Lin, "Synthesis of clathrate cerium superhydride CeH_9 at 80-100 GPa with atomic hydrogen sublattice," Nat. Commun. **10**(1), 4453 (2019).
[16]W. Chen, D. V. Semenok, X. Huang, H. Shu, X. Li, D. Duan, T. Cui, and A. R. Oganov, "High-temperature superconducting phases in cerium superhydride with a T_c up to 115 K below a pressure of 1 Megabar," Phys. Rev. Lett. **127**(11), 117001 (2021).
[17]D. V. Semenok, I. A. Troyan, A. G. Ivanova, A. G. Kvashnin, I. A. Kruglov, M. Hanfland, A. V. Sadakov, O. A. Sobolevskiy, K. S. Pervakov, I. S. Lyubutin, K. V. Glazyrin, N. Giordano, D. N. Karimov, A. L. Vasiliev, R. Akashi, V. M. Pudalov, and A. R. Oganov, "Superconductivity at 253 K in lanthanum–yttrium ternary hydrides," Mater. Today **48**, 18–28 (2021).
[18]H. Liu, I. I. Naumov, R. Hoffmann, N. W. Ashcroft, and R. J. Hemley, "Potential high-T_c superconducting lanthanum and yttrium hydrides at high pressure," Proc. Natl. Acad. Sci. U. S. A. **114**(27), 6990–6995 (2017).
[19]L. Ma, K. Wang, Y. Xie, X. Yang, Y. Wang, M. Zhou, H. Liu, X. Yu, Y. Zhao, H. Wang, G. Liu, and Y. Ma, "High-temperature superconducting phase in clathrate calcium hydride CaH_6 up to 215 K at a pressure of 172 GPa," Phys. Rev. Lett. **128**(16), 167001 (2022).
[20]Y. Qi, H. Lei, J. Guo, W. Shi, B. Yan, C. Felser, and H. Hosono, "Superconductivity in alkaline earth metal-filled skutterudites $Ba_xIr_4X_{12}$ (X = As, P)," J. Am. Chem. Soc. **139**(24), 8106–8109 (2017).
[21]O. Gunnarson, "Superconductivity in fullerides," Rev. Mod. Phys. **69**(2), 575 (1997).
[22]M. Mitrano, A. Cantaluppi, D. Nicoletti, S. Kaiser, A. Perucchi, S. Lupi, P. Di Pietro, D. Pontiroli, M. Riccò, S. R. Clark, D. Jaksch, and A. Cavalleri, "Possible light-induced superconductivity in K_3C_{60} at high temperature," Nature **530**(7591), 461–464 (2016).
[23]J. Guo, J.-i. Yamaura, H. Lei, S. Matsuishi, Y. Qi, and H. Hosono, "Superconductivity in $Ba_{n+2}Ir_{4n}Ge_{12n+4}$ (n = 1, 2) with cage structure and softening of low-lying localized mode," Phys. Rev. B **88**(14), 140507(R) (2013).
[24]S. Ishida, Y. Yanagi, K. Oka, K. Kataoka, H. Fujihisa, H. Kito, Y. Yoshida, A. Iyo, I. Hase, Y. Gotoh, and H. Eisaki, "Crystal structure and superconductivity of $BaIr_2Ge_7$ and $Ba_3Ir_4Ge_{16}$ with two-dimensional Ba-Ge networks," J. Am. Chem. Soc. **136**(14), 5245–5248 (2014).
[25]H. Duong Nguyen, Y. Prots, W. Schnelle, B. Böhme, M. Baitinger, S. Paschen, and Y. Grin, "Preparation, crystal structure and physical properties of the superconducting cage compound $Ba_3Ge_{16}Ir_4$," Z. Anorg. Allg. Chem. **640**(5), 760–767 (2014).
[26]Y. Zhao, J. Deng, A. Bhattacharyya, D. T. Adroja, P. K. Biswas, L. Gao, W. Cao, C. Li, C. Pei, T. Ying, H. Hosono, and Y. Qi, "Superconductivity in the layered cage compound $Ba_3Rh_4Ge_{16}$," Chin. Phys. Lett. **38**(12), 127402 (2021).
[27]C. Pei, T. Ying, Q. Zhang, X. Wu, T. Yu, Y. Zhao, L. Gao, C. Li, W. Cao, Q. Zhang, A. P. Schnyder, L. Gu, X. Chen, H. Hosono, and Y. Qi, "Caging-pnictogen-induced superconductivity in skutterudites IrX_3 (X = As, P)," J. Am. Chem. Soc. **144**, 6208 (2022).
[28]C. Pei, S. Jin, P. Huang, A. Vymazalova, L. Gao, Y. Zhao, W. Cao, C. Li, P. Nemes-Incze, Y. Chen, H. Liu, G. Li, and Y. Qi, "Pressure-induced superconductivity and structure phase transition in Pt_2HgSe_3," Npj Quantum Mater. **6**, 98 (2021).
[29]C. Pei, W. Shi, Y. Zhao, L. Gao, J. Gao, Y. Li, H. Zhu, Q. Zhang, N. Yu, C. Li, W. Cao, S. A. Medvedev, C. Felser, B. Yan, Z. Liu, Y. Chen, Z. Wang, and Y. Qi, "Pressure-induced a partial disorder and superconductivity in quasi-one-dimensional Weyl semimetal $(NbSe_4)_2I$," Mater. Today Phys. **21**, 100509 (2021).
[30]Q. Wang, P. Kong, W. Shi, C. Pei, C. Wen, L. Gao, Y. Zhao, Q. Yin, Y. Wu, G. Li, H. Lei, J. Li, Y. Chen, S. Yan, and Y. Qi, "Charge density wave orders and enhanced superconductivity under pressure in the kagome metal CsV_3Sb_5," Adv. Mater. **33**, 2102813 (2021).
[31]C. Pei, Y. Xia, J. Wu, Y. Zhao, L. Gao, T. Ying, B. Gao, N. Li, W. Yang, D. Zhang, H. Gou, Y. Chen, H. Hosono, G. Li, and Y. Qi, "Pressure-induced topological and structural phase transitions in an antiferromagnetic topological insulator," Chin. Phys. Lett. **37**(6), 066401 (2020).
[32]C. Pei and L. Wang, "Recent progress on high-pressure and high-temperature studies of fullerenes and related materials," Matter Radiat. Extremes **4**(2), 028201 (2019).
[33]H. K. Mao, J. Xu, and P. M. Bell, "Calibration of the ruby pressure gauge to 800 kbar under quasi-hydrostatic conditions," J. Geophys. Res.: Solid Earth **91**(B5), 4673–4676, https://doi.org/10.1029/jb091ib05p04673 (1986).
[34]A. P. Hammersley, S. O. Svensson, M. Hanfland, A. N. Fitch, and D. Hausermann, "Two-dimensional detector software: From real detector to idealised image or two-theta scan," High Pressure Res. **14**(4–6), 235 (1996).
[35]A. C. Larson and R. B. V. Dreele, "General structure analysis system (GSAS)," Los Alamos National Laboratory Report LAUR No. 86, 2004.
[36]B. H. Toby, "*EXPGUI*, a graphical user interface for *GSAS*," J. Appl. Crystallogr. **34**(2), 210 (2001).
[37]L. Sun, X.-J. Chen, J. Guo, P. Gao, Q.-Z. Huang, H. Wang, M. Fang, X. Chen, G. Chen, Q. Wu, C. Zhang, D. Gu, X. Dong, L. Wang, K. Yang, A. Li, X. Dai, H.-k. Mao, and Z. Zhao, "Re-emerging superconductivity at 48 kelvin in iron chalcogenides," Nature **483**(7387), 67–69 (2012).
[38]J. P. Sun, P. Shahi, H. X. Zhou, Y. L. Huang, K. Y. Chen, B. S. Wang, S. L. Ni, N. N. Li, K. Zhang, W. G. Yang, Y. Uwatoko, G. Xing, J. Sun, D. J. Singh, K. Jin, F. Zhou, G. M. Zhang, X. L. Dong, Z. X. Zhao, and J.-G. Cheng, "Reemergence of high-T_c superconductivity in the $(Li_{1-x}Fe_x)OHFe_{1-y}Se$ under high pressure," Nat. Commun. **9**(1), 380 (2018).
[39]C. Huang, J. Guo, K. Zhao, F. Cui, S. Qin, Q. Mu, Y. Zhou, S. Cai, C. Yang, S. Long, K. Yang, A. Li, Q. Wu, Z. Ren, J. Hu, and L. Sun, "Reemergence of superconductivity in pressurized quasi-one-dimensional superconductor $K_2Mo_3As_3$," Phys. Rev. Mater. **5**(2), L021801 (2021).
[40]Y. Zhou, X. Chen, R. Zhang, J. Shao, X. Wang, C. An, Y. Zhou, C. Park, W. Tong, L. Pi, Z. Yang, C. Zhang, and Y. Zhang, "Pressure-induced reemergence of superconductivity in topological insulator $Sr_{0.065}Bi_2Se_3$," Phys. Rev. B **93**(14), 144514 (2016).

[41] C. C. Zhu, X. F. Yang, W. Xia, Q. W. Yin, L. S. Wang, C. C. Zhao, D. Z. Dai, C. P. Tu, B. Q. Song, Z. C. Tao, Z. J. Tu, C. S. Gong, H. C. Lei, Y. F. Guo, and S. Y. Li, "Double-dome superconductivity under pressure in the V-based Kagome metals AV_3Sb_5 (A = Rb and K)," Phys. Rev. B **105**(9), 094507 (2022).

[42] X. Chen, X. Zhan, X. Wang, J. Deng, X.-B. Liu, X. Chen, J.-G. Guo, and X. Chen, "Highly robust reentrant superconductivity in CsV_3Sb_5 under pressure," Chin. Phys. Lett. **38**(5), 057402 (2021).

[43] Z. Zhang, Z. Chen, Y. Zhou, Y. Yuan, S. Wang, J. Wang, H. Yang, C. An, L. Zhang, X. Zhu, Y. Zhou, X. Chen, J. Zhou, and Z. Yang, "Pressure-induced reemergence of superconductivity in the topological kagome metal CsV_3Sb_5," Phys. Rev. B **103**(22), 224513 (2021).

[44] C. K. Jones, J. K. Hulm, and B. S. Chandrasekhar, "Upper critical field of solid solution alloys of the transition elements," Rev. Mod. Phys. **36**(1), 74–76 (1964).

[45] J. A. Woollam, R. B. Somoano, and P. O'Connor, "Positive curvature of the H_{c2}-versus-T_c boundaries in layered superconductors," Phys. Rev. Lett. **32**(13), 712–714 (1974).

[46] F. Birch, "Finite elastic strain of cubic crystals," Phys. Rev. **71**(11), 809–824 (1947).